This is a repository copy of *Coupling of single quantum dots to photonic crystal cavities investigated by low-temperature scanning near-field optical microscopy*.

White Rose Research Online URL for this paper:
http://eprints.whiterose.ac.uk/78954/

Version: Published Version

Article:

Coupling of single quantum dots to photonic crystal cavities investigated by low-temperature scanning near-field optical microscopy

Matthias Skacel,[1] Francesco Pagliano,[1,*] Thang Hoang,[1] Leonardo Midolo,[1] Sartoon Fattahpoor,[1] Lianhe Li,[2] Edmund H. Linfield,[2] and Andrea Fiore[1]

[1]*COBRA Research Institute, Eindhoven University of Technology, 5600 MB Eindhoven, The Netherlands*
[2]*School of Electronic and Electrical Engineering, University of Leeds, Leeds LS2 9JT, United Kingdom*

We report a study of single quantum dots inside photonic crystal cavities with a low-temperature scanning near-field optical microscope. The spatial maps of single excitonic lines from the quantum dot show the clear signature of coupling to the cavity modes for small detunings. We also show that the near-field tip can be used to control the exciton-photon coupling at the nanoscale. A general framework for the interpretation of near-field maps of single emitters in cavities is proposed.

I. INTRODUCTION

Solid-state cavity quantum electrodynamic (CQED) systems are of major interest for future quantum communication applications. Quantum dots (QDs) in photonic crystal (PhC) cavities have been shown to be a good candidate for the realization of practical implementations of CQED,[1] for example as efficient single-photon sources.

In order to make use of the discretized energy levels of QDs, it is necessary to study them at low temperature. Microphotoluminescence spectroscopy (μPL), with additional time correlated single photon counting or two-photon correlation measurements, is the most popular method for studying the optical properties of single QDs and PhC cavities. However, μPL lacks the spatial resolution needed to study the spatial coupling between QD and PhC cavity, which plays a key role in parameters such as the Rabi frequency and the Purcell factor. Scanning near-field optical microscopy (SNOM) has been used to characterize PhC cavities at room temperature[2–8] and single QDs at low temperatures.[9–12] However, near-field studies of the coupling of single QDs to PhC cavity modes have not been reported so far. By performing such a near-field study, we demonstrate here that the interaction between QD, cavity mode and near-field tip leads to surprising observations. The complex interplay between the near-field tip and the cavity mode, together with the coupling of the excitonic QD emission to the cavity mode, leads to distinctly different spatial maps of the QD lines, depending on their spectral alignment to the cavity modes. We give an explanation for the observed results and show that near-field imaging provides an important insight on the QD-cavity coupling.

The sample under investigation contains low density ($\approx 10\ \mu m^{-2}$) InAs QDs emitting at 1300 nm at low temperature, grown by molecular beam epitaxy.[13] The QDs are grown in the center of a 320-nm thick GaAs membrane on top of a 1.5-μm AlGaAs sacrificial layer.[14] The pattern of the PhC cavity was transferred onto the sample by electron beam lithography and subsequent inductively coupled plasma etching. To form a cavity, one hole of a hexagonal PhC is removed. The first row of holes surrounding the cavity is reduced in size and shifted in position in order to increase the quality factor.[15] Such modified H1 cavity is interesting

for SNOM experiments due to the existence of several modes with different spatial pattern. The topography of one of these cavities is shown as inset in Fig. 1.

For the measurements presented here, we have built a tuning fork-based low-temperature SNOM employing the excitation-collection mode. Photoluminescence (PL) is nonresonantly excited through an uncoated fiber tip using a 750-nm pulsed diode laser with a pulse width of 200 ps and a repetition rate of 20 MHz. The PL is collected from the same tip, dispersed by a 0.55-m spectrometer and analyzed by a liquid nitrogen cooled InGaAs charge coupled device (CCD). For scanning and positioning, we use piezos and steppers from *attocube systems*. The sample, the piezos, and the tuning fork are inside a flowing vapor cryostat from Janis Research in the flow of cold Helium gas at 7 K. We employ uncoated fiber tips since coated tips have too low transmission for single dot spectroscopy. As shown below, the use of uncoated tips and the very low signal levels intrinsically related to single QD spectroscopy limit the spatial resolution in our experiment but do not prevent the observation of the tip-induced perturbation of the QD-cavity interaction, which leads to novel and surprising insights.[16] After approaching the tip to 5–10 nm distance from the sample, it is scanned along the surface. At each point during an image scan, the tip is stopped and a spectrum is acquired. The obtained spectra are then rearranged to show an image for each wavelength.

We first present a case where the QD excitonic lines are far detuned from the cavity modes. Figure 1 shows the spectrum of such a cavity (cavity A) with 14 μW average pump power in the fiber. It shows two distinct sharp lines marked with X and XX, two cavity modes marked with M1 and M2, with quality factors $Q = 860$ and 1290, respectively, and several weaker lines. By taking power-dependent spectra (not shown here), X and XX were identified as the exciton and biexciton emission of the same QD. The PL maps of X and XX are shown in Figs. 2(a) and 2(b), respectively. It is apparent that both lines originate in the same location, confirming our attribution that they originate from the same QD. Additionally, we observe a circular shape, which is not significantly influenced by the PhC cavity. We remark that the QDs are buried 160 nm below the surface in the center of the slab and therefore the QD emission
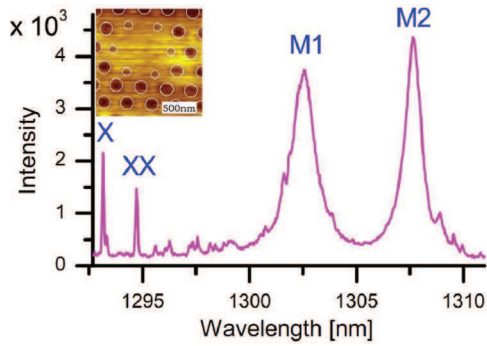
FIG. 1. (Color online) SNOM spectrum of cavity A acquired with the tip positioned at the cavity center at 7 K with a pump power of 14 μW. (Inset) Topography acquired during the image scan. The holes of the PhC are drawn as white circles to guide the eye.

results in a relatively large spot of 600-nm full-width at half maximum, much larger than usually observed for QDs close to the surface,[17] but similar to previously reported maps of buried QDs.[10]

Figure 3(a) [Fig. 3(c)] shows the PL intensity maps of the cavity mode M1 (M2) in Fig. 1. These are the quasidegenerate quadrupole modes of the modified H1 cavity as determined by taking μPL spectra prior to the SNOM measurements and comparing with literature.[15] The degeneracy is split due to fabrication imperfections. The intensity collected by the tip is expected to map the modulus square of the in-plane electric field at the surface of the membrane.[18] Figures 3(b) and 3(d) show the modulus square of the in-plane electric field for modes M1 and M2, respectively, calculated using a 2D finite element software. The observed mode maps are clearly elongated along the two orthogonal axes of the cavity, in agreement with the calculation. However, the fine features of the calculated mode patterns are not resolved, as it was already observed in room-temperature SNOM of PhC cavities with high-density QDs.[5] This is a consequence of the limited spatial resolution of the tip. Convolving the calculated mode profile with a Gaussian-shaped instrument response function (IRF) with full width half maximum (FWHM) of 200 nm provides a closer match with the experimental data (not shown). This gives an estimation of the spatial resolution of our SNOM images, as observed in room-temperature experiments.[18] However, since a generally accepted model for the IRF is not available, we consider only the calculated mode profile in the following. Additionally, in the present case of
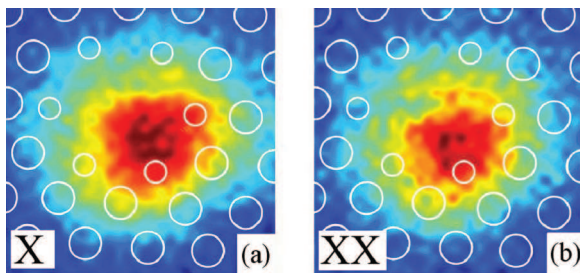

FIG. 2. (Color online) Maps of the X and XX emissions collected at $\lambda = 1293.2$ and 1294.7 nm, respectively, for a pump power of 14 μW.
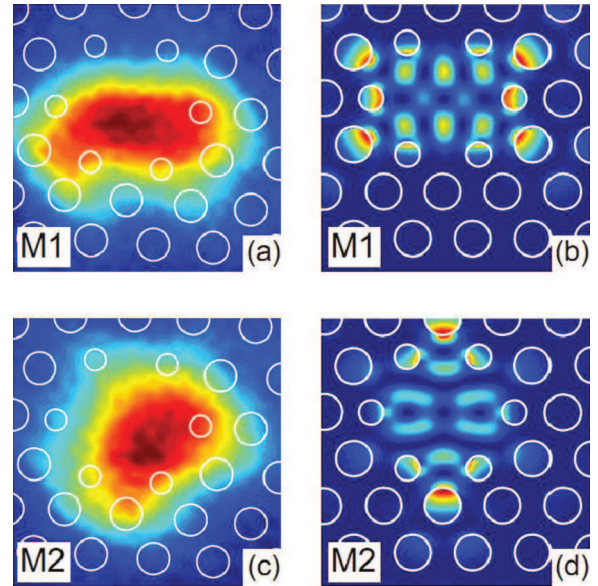

FIG. 3. (Color online) (a) Intensity PL map of M1, (b) calculated modulus square of the electric field of M1, (c) intensity PL map of M2, and (d) calculated modulus square of the electric field of M2.

low-density QDs, where only one QD is present in the cavity, we expect that in the employed illumination-collection mode the pumping of the QD strongly depends on the tip position, producing substantial changes to the map. Indeed, this explain why the PL map presents a maximum just below the cavity center, corresponding to the position of the QD as observed from the maps in Fig. 2. We note that for this large detuning the modes are pumped by a broad background corresponding to multiexcitonic transitions in the QD.[19–21] The observed optical maps result from the combined effect of spatial-dependent pumping and collection, as detailed below.

Figure 4 shows the spectrum of another cavity (cavity B), whose topography is shown as inset, taken with the tip positioned at the center of the cavity. When the tip is approached (lower magenta line), it shows a biexcitonic peak XX at 1280.2 nm and a cavity mode M at 1279.15 nm. When the tip is retracted (upper, cyan line), the mode blue shifts by 0.14 nm, while the XX peak remains unaffected.
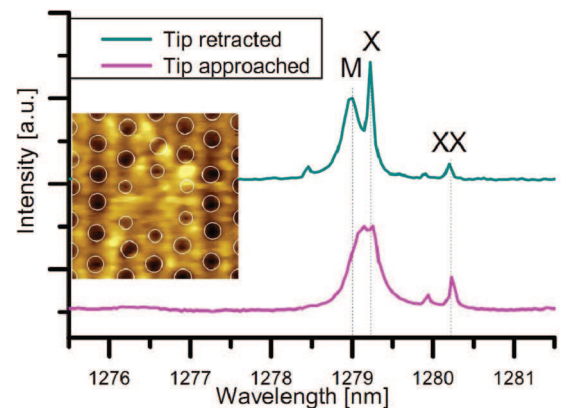

FIG. 4. (Color online) Near-field PL spectrum of cavity B with tip approached (lower, magenta line) and tip retracted (upper, cyan line).
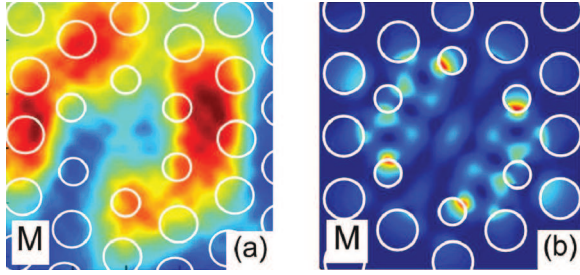
FIG. 5. (Color online) (a) Intensity PL map of M. (b) Calculated modulus square of the electric field of mode M.

Additionally, it becomes apparent that there is an excitonic line X at 1279.2 nm in resonance with the mode. This is an easy method to distinguish excitonic lines from cavity modes by SNOM; due to the dielectric perturbation produced by the tip,[5,22] the cavity modes shift when the tip is approached whereas excitonic lines are unaffected. In order to separate the contribution of QD lines and cavity mode, we fit the acquired spectra with a sum of Lorentzians,

$$S(\lambda, x, y) = y_0(x, y) + \sum_{i=X,XX,M} \frac{A_i(x,y) w_i}{2\pi [(\lambda - \lambda_{0,i}(x,y)]2 + w_i{}^2/4)},$$

$$(1)$$

keeping w_i fixed and fitting the peak amplitudes $A_i(x,y)$ and $\lambda_{0,i}(x,y)$ for each spatial position (x,y) of the tip. For the QD lines, we keep $\lambda_{0,i}(x,y)$ fixed. The obtained intensity map of M is shown in Fig. 5(a). As determined by taking a room-temperature μPL spectrum (not shown here) over a wide spectral range and identifying the modes of the modified H1 cavity type, the observed mode is one of the two quasidegenerate second-order dipole modes[15] whose degeneracy is split due to manufacturing imperfections. The second mode of the two is observed at 1274.5 nm, outside the spectral range shown in Fig. 4. The calculated mode profile is shown in Fig. 5(b).

We now focus on the spatial coupling of the QD lines to mode M. To this aim, the maps $A_X(x,y)$ and $A_{XX}(x,y)$ of the intensity of X and XX lines are shown in Figs. 6(a) and 6(b), respectively. Looking first at line XX, which is more detuned from the mode, we observe that surprisingly its intensity map shows more similarity with mode M than with a circular shape of a QD. This is caused by the coupling of the XX line to the cavity mode, and the modification of this coupling induced by the tip-induced shift of M. As described above, the mode shifts due to the perturbation by the tip. This leads to a change of the
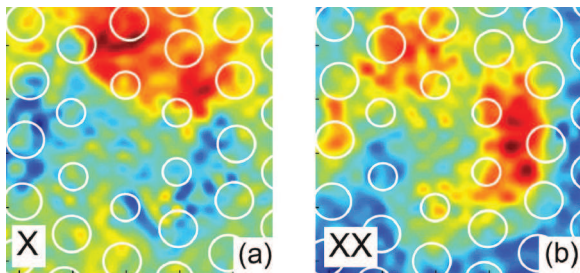

FIG. 6. (Color online) Intensity maps of (a) X and (b) XX for cavity B.

spectral mismatch term F_{cav} of the Purcell formula:[23]

$$F_{cav}(\lambda_M) = \frac{1}{1 + 4Q^2 \left(\frac{\lambda_{QD}}{\lambda_M} - 1\right)^2},$$

$$(2)$$

where λ_M, λ_{QD} are the wavelenghts of cavity mode and QD, respectively, and Q is the mode quality factor ($Q = 4200$). At the spectral position of XX, the calculated spectral mismatch term varies by a factor of $7.1\times$, depending on whether the tip is at a maximum or minimum of the mode. The peculiar shape of the XX maps shows that even if the QD is detuned from the mode by several linewidths, there is coupling between them. We stress that this represents a clear evidence of coupling, which is unique to this near-field technique.

On the contrary, the intensity map of line X [see Fig. 6(a)] shows a lobe in the upper part and a negative, blue imprint of the cavity mode. We interpret this as a consequence of the tip-induced detuning of the cavity from the X line. We note that the spectra in Fig. 4 were taken with the tip in the center of the cavity. Since the electric field at this position is weak, the perturbation is not as strong as when the tip is in a region of high mode strength. Therefore, in the regions with high electric field, the mode is on the long wavelength side of X. As the tip gets into a region of high mode strength, the mode shifts towards the red, thereby reducing the Purcell effect on X and producing the blue negative imprint.

In general, the PL collected by the tip at the emission wavelength of QD lines has two contributions: first, the PL emitted into leaky modes of the PhC, and second, the PL coupled to the cavity mode and subsequently scattered into the fiber tip. The first term is proportional to $N_{exc}(x,y)\, \gamma_{leak}^{QD}\, \eta_{leak}^{coll}(x,y)$, whereas the second term has a spatial dependence proportional to $N_{exc}(x,y)\, \gamma_{mode}^{QD}\, F_{cav}[\lambda_M(x,y)]\, \eta_M^{coll}(x,y)$, where $N_{exc}(x,y)$ is the number of carriers injected in the QD when the tip is positioned at x and y, which depends on the distribution of pump power produced by the tip, on the absorption and on the carrier diffusion length. γ_{leak}^{QD} is the QD emission rate into leaky modes in the PhC band gap[24] and γ_{mode}^{QD} is the QD emission rate into cavity mode M at resonance ($\lambda_{QD} = \lambda_M$). $F_{cav}[\lambda_M(x,y)]$ is the spectral coupling term [in Eq. (2)], which depends on the position of the tip in the mode pattern. Finally, $\eta_{leak}^{coll}(x,y)$ and $\eta_{mode}^{coll}(x,y)$ are the collection efficiencies of the tip for leaky modes and mode M, respectively, when the tip is positioned at (x,y). They are expected to follow the $|E|^2$ mode pattern, neglecting a possibly asymmetric tip geometry or contribution of far-field components.[5] The fields collected through these two channels may also interfere, but in the following we will consider situations where a single contribution is dominant and therefore the interference can be neglected.

In the case of cavity A, X, and XX are strongly detuned from the mode. Therefore F_{cav} is negligibly small and all emission occurs into leaky modes of the PhC. Thus the observed intensity maps reproduce the $N_{exc}(x,y)\, \eta_{leak}^{coll}(x,y)$ term, as described above. When the tip is located on top of the QD, both $N_{exc}(x,y)$ and $\eta_{leak}^{coll}(x,y)$ are maximum and therefore the collected PL is maximum at the QD position. In the case of cavity B, the situation is different. Since X and XX are closer to M, the second term becomes dominant, as it is evident from the observation that the XX map closely resembles the cavity mode. While the $N_{exc}(x,y)$ and η_M^{coll} terms are the same in
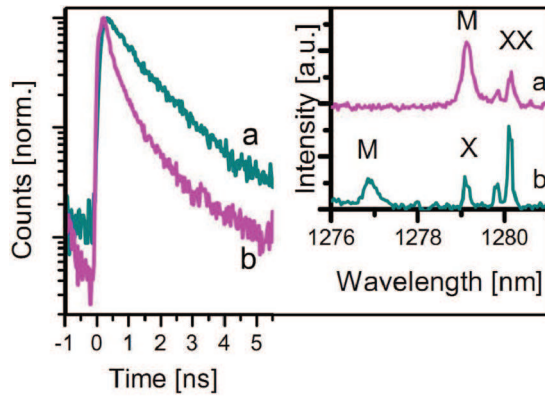
FIG. 7. (Color online) Time-resolved PL of XX (with the tip positioned in the center of the cavity and an excitation power of 50 nW) in two different cool-down runs, for a detuning of 1.05 nm (magenta trace), and a detuning of 3.35 nm (green trace). (Inset) Corresponding spectra in the two cool-down runs. Note that in case b cavity mode M is blue shifted by 2.4 nm compared to case a.

the X and XX maps, the $F_{cav}[\lambda_M(x,y)]$ term has an opposite effect: approaching the tip to a field-maximum redshifts λ_M, producing an increase of $F_{cav}[\lambda_M(x,y)]$ for the XX line and a decrease for the X line. This produces the blue imprint of the mode in the X map in Fig. 6(a). The difference in the X and XX maps therefore directly demonstrates the effect of the dielectric tip on the spontaneous emission rate of a QD in a cavity. We note that the X map in Fig. 6(a) presents a lobe in the upper part of the cavity. This is attributed to the influence of the $N_{exc}(x,y)$ term, which is maximum at the position of the QD. Indeed, imaging the broad background produced by the QD in a spectral region far from these lines,[25] we have determined that the QD in cavity B is positioned in this region. This also explains the asymmetry in the XX map, which also presents a larger intensity in the upper half.

In order to further support our conclusions, we have performed near-field time-correlated single-photon counting (TCSPC) using a superconducting single-photon detector (SSPD).[26] To this aim, the PL collected when the tip was positioned at the center of the cavity was spectrally filtered, sent to the SSPD, and the SSPD output signal correlated with a trigger pulse from the pump laser in a correlation card, resulting in a temporal resolution of 250 ps. The combined decay of M and X (not shown) gives two time constants of 280 ps and 1.65 ns, where we attribute the short one to

the cavity mode emission (pumped by the multiexcitonic background) and the long one to X decay time. The XX decay shows a dominant decay component with a time constant of 1.2 ns (magenta line in Fig. 7). In another cool-down run, when the cavity mode was blue shifted by 2.4 nm (see inset of Fig. 7), due to the changed environmental conditions, we have repeated the TCSPC in order to evaluate the change of F_{cav}. Now that both X and XX are detuned from M, they show a monoexponential decay with a lifetime of 3.1 and 5.0 ns for X and XX, respectively. Figure 7 shows the XX decay curve in this situation (green curve). The strong increase in the XX lifetime as its detuning from M is increased from 1.05 to 3.35 nm, clearly proves that at smaller detuning the coupling to the cavity mode is dominant and further corroborates our interpretation of the maps in Fig. 6.

In conclusion, we have presented a general framework for the interpretation of low-temperature SNOM of single QDs in PhC cavities. We have shown that the QD emission far off-resonant with a PhC mode has a circular shape, allowing the identification of the QD position inside the PhC. In contrast, when QD and PhC cavity modes come close to resonance, the mode is strongly affecting the intensity map of QD lines. When the excitonic line is on the long-wavelength side of the mode, its map takes the shape of the mode due to the influence of the tip-induced shift. If the excitonic line is on the short-wavelength side, its map shows signature of suppressed emission due to the tip-induced wavelength shift. Despite the limited resolution in the mapping of single QD lines, near-field PL mapping of QDs in PhC cavities therefore provides detailed information on their spatial and spectral coupling due to local dielectric perturbation produced by the tip. Additionally, these experiments demonstrate the possibility of controlling the spontaneous emission from a QD by nanomanipulation of a near-field tip.

*f.m.pagliano@tue.nl

[1] A. J. Shields, Nat Photon **1**, 215 (2007).

[2] D. Shin, S. Kim, J. Hwang, H. Ryu, H. Park, D. Song, and Y. Lee, Quantum Electronics, IEEE J. Quantum Electron. **38**, 857 (2002).

[3] D. Gérard, L. Berguiga, F. de Fornel, L. Salomon, C. Seassal, X. Letartre, P. Rojo-Romeo, and P. Viktorovitch, Opt. Lett. **27**, 173 (2002).

[4] K. Okamoto, M. Loncar, T. Yoshie, A. Scherer, Y. Qiu, and P. Gogna, Appl. Phys. Lett. **82**, 1676 (2003).

[5] F. Intonti, S. Vignolini, F. Riboli, A. Vinattieri, D. S. Wiersma, M. Colocci, L. Balet, C. Monat, C. Zinoni, L. H. Li, R. Houdre, M. Francardi, A. Gerardino, A. Fiore, and M. Gurioli, Phys. Rev. B **78**, 041401 (2008).

[6] S. Vignolini, F. Intonti, F. Riboli, D. S. Wiersma, L. Balet, L. H. Li, M. Francardi, A. Gerardino, A. Fiore, and M. Gurioli, Appl. Phys. Lett. **94**, 163102 (2009).

[7] M. Burresi, T. Kampfrath, D. van Oosten, J. C. Prangsma, B. S. Song, S. Noda, and L. Kuipers, Phys. Rev. Lett. **105**, 123901 (2010).

[8]S. Vignolini, F. Intonti, F. Riboli, L. Balet, L. H. Li, M. Francardi, A. Gerardino, A. Fiore, D. S. Wiersma, and M. Gurioli, Phys. Rev. Lett. **105**, 123902 (2010).

[9]Y. Toda, M. Kourogi, M. Ohtsu, Y. Nagamune, and Y. Arakawa, Appl. Phys. Lett. **69**, 827 (1996).

[10]D. Pahlke, I. Manke, F. Heinrichsdorff, M. Dähne-Prietsch, and W. Richter, Appl. Surf. Sci. **123–124**, 400 (1998).

[11]G. Guttroff, M. Bayer, A. Forchel, D. V. Kazantsev, M. K. Zundel, and K. Eberl, Phys. Status Solidi (a) **164**, 291 (1997).

[12]A. Mintairov, Y. Tang, J. Merz, V. Tokranov, and S. Oktyabrsky, Phys. Status Solidi (c) **2**, 845 (2005).

[13]B. Alloing, C. Zinoni, V. Zwiller, L. H. Li, C. Monat, M. Gobet, G. Buchs, A. Fiore, E. Pelucchi, and E. Kapon, Appl. Phys. Lett. **86**, 101908 (2005).

[14]L. Balet, M. Francardi, A. Gerardino, N. Chauvin, B. Alloing, C. Zinoni, C. Monat, L. Li, N. Le Thomas, R. Houdré, and A. Fiore, Appl. Phys. Lett. **91**, 123115 (2007).

[15]M. Shirane, S. Kono, J. Ushida, S. Ohkouchi, N. Ikeda, Y. Sugimoto, and A. Tomita, J. Appl. Phys. **101**, 073107 (2007).

[16]A. Crottini, Ph.D. thesis, Ecole Polytechnique Federale de Lausanne, 2001.

[17]K. Matsuda, T. Saiki, S. Nomura, M. Mihara, Y. Aoyagi, S. Nair, and T. Takagahara, Phys. Rev. Lett. **91**, 177401 (2003).

[18]F. Intonti, S. Vignolini, F. Riboli, A. Vinattieri, D. Wiersma, M. Colocci, M. Gurioli, L. Balet, C. Monat, L. Li, N. Le Thomas, R. Houdré, A. Fiore, M. Francardi, A. Gerardino, F. Roemer, and B. Witzigmann, Phys. E **40**, 1965 (2008).

[19]A. Laucht, M. Kaniber, A. Mohtashami, N. Hauke, M. Bichler, and J. J. Finley, Phys. Rev. B **81**, 241302 (2010).

[20]M. Winger, T. Volz, G. Tarel, S. Portolan, A. Badolato, K. J. Hennessy, E. L. Hu, A. Beveratos, J. Finley, V. Savona, and A. Imamoglu, Phys. Rev. Lett. **103**, 207403 (2009).

[21]N. Chauvin, C. Zinoni, M. Francardi, A. Gerardino, L. Balet, B. Alloing, L. H. Li, and A. Fiore, Phys. Rev. B **80**, 241306 (2009).

[22]A. F. Koenderink, M. Kafesaki, B. C. Buchler, and V. Sandoghdar, Phys. Rev. Lett. **95**, 153904 (2005).

[23]D. Englund, D. Fattal, E. Waks, G. Solomon, B. Zhang, T. Nakaoka, Y. Arakawa, Y. Yamamoto, and J. Vučković, Phys. Rev. Lett. **95**, 013904 (2005).

[24]A. Kress, F. Hofbauer, N. Reinelt, M. Kaniber, H. J. Krenner, R. Meyer, G. Böhm, and J. J. Finley, Phys. Rev. B **71**, 241304 (2005).

[25]M. Skacel, F. Pagliano, T. B. Hoang, L. Midolo, S. Fattahpoor, L. Li, E. Linfield, and A. Fiore (unpublished).

[26]C. Zinoni, B. Alloing, C. Monat, V. Zwiller, L. H. Li, A. Fiore, L. Lunghi, A. Gerardino, H. de Riedmatten, H. Zbinden, and N. Gisin, Appl. Phys. Lett. **88**, 131102 (2006).